Tiana, J. [et al.] (2018) Experimental study of modulation waveforms for entraining the spikes emitted by a semiconductor laser with optical feedback. *Optics express*. Vol. 26, issue 7, p. 9298-9309. DOI: 10.1364/OE.26.009298

Research Article | Vol. 26, No. 7 | 2 Apr 2018 | OPTICS EXPRESS 9298
Optics EXPRESS

Experimental study of modulation waveforms for entraining the spikes emitted by a semiconductor laser with optical feedback

J. TIANA-ALSINA,[1] C. QUINTERO-QUIROZ,[1] M. PANOZZO,[1,2] M. C. TORRENT,[1] AND C. MASOLLER[1,*]

[1] *Universitat Politècnica de Catalunya, Departament de Física, Rambla St. Nebridi 22, 08222 Terrassa, Barcelona, Spain*
[2] *Università degli Studi di Padova, Italy*
[*] *cristina.masoller@upc.edu*

Abstract: The entrainment phenomenon, by which an oscillator adjusts its natural rhythm to an external periodic signal, has been observed in many natural systems. Recently, attention has focused on which are the optimal conditions for achieving entrainment. Here we use a semiconductor laser with optical feedback, operating in the low-frequency fluctuations (LFFs) regime, as a testbed for a controlled entrainment experiment. In the LFF regime the laser intensity displays abrupt spikes, which can be entrained to a weak periodic signal that directly modulates the laser pump current. We compare the performance of three modulation waveforms for producing 1:1 locking (one spike is emitted in each modulation cycle), as well as higher order locking regimes. We characterize the parameter regions where high-quality locking occurs, and those where the laser emits spikes which are not entrained to the external signal. The role of the modulation amplitude and frequency, and the role of the dc value of the laser pump current (that controls the natural spike frequency) in the entrainment quality are discussed.

OCIS codes: (140.1540) Chaos; (140.5960) Semiconductor lasers; (250.5960) Semiconductor lasers

References and links

1. A. Pikovsky, M. Rosenblum, and J. Kurths, *Synchronization: A universal concept in nonlinear sciences* (Cambridge University Press, 2001).
2. T. Harada, H.A. Tanaka, M.J. Hankins and I.Z. Kiss, "Optimal waveform for the entrainment of a weakly forced oscillator," Phys. Rev. Lett. **105**, 088301 (2010).
3. A.E. Granada and H. Herzel, "How to achieve fast entrainment? The timescale to synchronization," PLoS ONE **4**(9): e7057 (2009).
4. A. Zlotnik, Y. Chen, I.Z. Kiss, H.A. Tanaka, and J.S. Li, "Optimal waveform for fast entrainment of weakly forced nonlinear oscillators," Phys. Rev. Lett. **111**, 024102 (2013).
5. A. Pikovsky, "Maximizing coherence of oscillations by external locking," Phys. Rev. Lett. **115**, 070602 (2015).
6. H.A. Tanaka, "Optimal entrainment with smooth, pulse, and square signals in weakly forced nonlinear oscillator," Physica D **288**, 1–22 (2014).
7. J. Mork, B. Tromborg and J. Mark, "Chaos in semiconductor lasers with optical feedback – Theory and experiment," IEEE J. Quantum Electron. **28**, 93–108 (1992).
8. J. Ohtsubo, *Semiconductor Lasers, Stability, Instability and Chaos* (Springer, 3th edition, 2013)
9. M. Sciamanna and K. A. Shore, "Physics and applications of laser diode chaos," Nat. Photonics **9**, 151 (2015).
10. L. Jumpertz, K. Schires, M. Carras, M. Sciamanna, and F. Grillot, "Chaotic light at mid-infrared wavelength," Light-Science & Appl. 5, e16088 (2016).
11. J. X. Dong, J. P. Zhuang, and S.-C. Chan, "Tunable switching between stable and periodic states in a semiconductor laser with feedback," Opt. Lett. 42, 4291–4294 (2017).
12. T. Sano, "Antimode dynamics and chaotic itinerancy in the coherence collapse of semiconductor lasers with optical feedback," Phys. Rev. A **50**, 2719–2726 (1994).
13. A. Hohl, H.J.C. Vanderlinden, and R. Roy, "Determinism and stochasticity of power-dropout events in semiconductor-lasers with optical feedback," Opt. Lett. **20**, 2396–2398 (1995).
14. I. Fischer, G.H.M. van Tartwijk, A.M. Levine, W. Elsasser, E. Gobel, and D. Lenstra, "Fast pulsing and chaotic itinerancy with a drift in the coherence collapse of semiconductor lasers," Phys. Rev. Lett. **76**, 220 (1996).
15. D.W. Sukow, J.R. Gardner, and D.J. Gauthier, "Statistics of power-dropout events in semiconductor lasers with time-delayed optical feedback," Phys. Rev. A **56**, R3370–R3373 (1997).

#323041 https://doi.org/10.1364/OE.26.009298
Journal © 2018 Received 14 Feb 2018; revised 21 Mar 2018; accepted 26 Mar 2018; published 30 Mar 2018

Optics EXPRESS

16. T. Heil, I. Fischer, W. Elsasser, J. Mulet, and C.R. Mirasso, "Statistical properties of LFFs during single-mode operation in distributed-feedback lasers: experiments and modeling," Opt. Lett. **24**, 1275–1277 (1999).
17. R.L. Davidchack, Y.C. Lai, A. Gavrielides, and V. Kovanis, "Dynamical origin of low frequency fluctuations in external cavity semiconductor lasers," Phys. Lett. A **267**, 350–356 (2000).
18. G. Giacomelli, M. Giudici, S. Balle, and J. R. Treddice, "Experimental evidence of coherence resonance in an optical system," Phys. Rev. Lett. **84**, 3298–3301 (2000).
19. J. F. M. Avila, H. L. D. S. Cavalcante, and J. R. R. Leite, "Experimental deterministic coherence resonance," Phys. Rev. Lett. **93**, 144101 (2004).
20. Y. Hong and K.A. Shore, "Statistical measures of the power dropout ratio in semiconductor lasers subject to optical feedback," Opt. Lett. **30**, 3332–3334 (2005).
21. J. Tiana-Alsina, M.C. Torrent, O.A. Rosso, C. Masoller, J. García-Ojalvo, "Quantifying the statistical complexity of low-frequency fluctuations in semiconductor lasers with optical feedback," Phys. Rev. A **82**, 013819 (2010).
22. T. Schwalger, J. Tiana-Alsina, M.C. Torrent, J. García-Ojalvo, and B. Lindner, "Interspike-interval correlations induced by two-state switching in an excitable system," EPL **99**, 10004 (2012).
23. D. Brunner, M. C. Soriano, X. Porte, and I. Fischer, "Experimental phase space tomography of semiconductor laser dynamics," Phys. Rev. Lett **115**, 053901 (2015).
24. F. Baladi, M.W. Lee, J-R Burie, M.A. Tettiati, A. Boudrioua, A.P.A. Fischer, "High-resolution LFF map of a multimode laser diode subject to filtered optical feedback via a fiber Bragg grating", Opt. Lett. **41**, 2950 (2016).
25. D. Choi, M.J. Wishon, J. Barnoud, C.Y. Chang, Y. Bouazizi, A. Locquet, and D. S. Citrin, "Low-frequency fluctuations in an external-cavity laser leading to extreme events," Phys. Rev. E **93**, 042216 (2016).
26. R. Lang and K. Kobayashi, "External optical feedback effects on semiconductor injection laser properties," IEEE J. Quantum Electron. **16**, 347–355 (1980).
27. A. Torcini, S. Barland, G. Giacomelli, and F. Marin, "Low-frequency fluctuations in vertical cavity lasers: Experiments versus Lang-Kobayashi dynamics," Phys. Rev. A **74**, 063801 (2006).
28. J. Zamora-Munt, C. Masoller, and J. García-Ojalvo, "Transient low-frequency fluctuations in semiconductor lasers with optical feedback," Phys. Rev. A **81**, 033820 (2010).
29. K. Hicke, X. Porte, and I. Fischer, "Characterizing the deterministic nature of individual power dropouts in semiconductor lasers subject to delayed feedback," Phys. Rev. E **88**, 052904 (2013).
30. A. Aragoneses, N. Rubido, J. Tiana-Alsina, M.C. Torrent, and C. Masoller, "Distinguishing signatures of determinism and stochasticity in spiking complex systems," Sci. Rep. **3**, 1778 (2013).
31. D.W. Sukow and D.J. Gauthier, "Entraining power-dropout events in an external-cavity semiconductor laser using weak modulation of the injection current," IEEE J. Quantum Electron. **36**, 175–183 (2000).
32. J.M. Mendez, R. Laje, M. Giudici, J. Aliaga, and G.B. Mindlin, "Dynamics of periodically forced semiconductor laser with optical feedback," Phys. Rev. E **63**, 066218 (2001).
33. J. P. Toomey, D. M. Kane, M. W. Lee, and K. A. Shore, "Nonlinear dynamics of semiconductor lasers with feedback and modulation," Opt. Express **18**, 16955 (2010).
34. D. Baums, W. Elsasser, and E.O. Gobel, "Farey tree and devils staircase of a modulated external-cavity semiconductor laser," Phys. Rev. Lett. **63**, 155–158 (1989).
35. J. Sacher, D. Baums, P. Panknin, W. Elsasser, and E.O. Gobel, "Intensity instabilities of semiconductor-lasers under current modulation, external light injection and delayed feedback," Phys. Rev. A **45**, 1893–1905 (1992).
36. F. Marino, M. Giudici, S. Barland, and S. Balle, "Experimental evidence of stochastic resonance in an excitable optical system," Phys. Rev. Lett. **88**, 040601 (2002).
37. L. Gammaitoni, P. Hanggi, P. Jung, and F. Marchesoni, "Stochastic resonance," Rev. Mod. Phys. **70**, 223–287 (1998).
38. T. Sorrentino, C. Quintero-Quiroz, A. Aragoneses, M. C. Torrent, and C. Masoller, "Effects of periodic forcing on the temporally correlated spikes of a semiconductor laser with feedback," Opt. Express **23**, 5571 (2015).
39. T. Sorrentino, C. Quintero-Quiroz, M.C. Torrent, and C. Masoller, "Analysis of the spike rate and spike correlations in modulated semiconductor lasers with optical feedback," IEEE J. Sel. Top. Quantum Electron. **21**, 1801107 (2015).
40. C. Quintero-Quiroz, J. Tiana-Alsina, J. Romà, M. C. Torrent, and C. Masoller, "Characterizing how complex optical signals emerge from noisy intensity fluctuations," Sci. Rep. **6** 37510 (2016).
41. M. Panozzo, C. Quintero-Quiroz, J. Tiana-Alsina, M. C. Torrent, and C. Masoller, "Experimental characterization of the transition to coherence collapse in a semiconductor laser with optical feedback," Chaos **27**, 114315 (2017).
42. Video showing how the intensity time series gradually changes as the laser pump current is increased: https://youtu.be/nltBQG_IIWQ.
43. T. Jin, C. Siyu, and C. Masoller, "Generation of extreme pulses on demand in semiconductor lasers with optical injection," Opt. Express **25**, 031326 (2017).

1. Introduction

The entrainment, or "locking" phenomenon, by which an oscillator adjusts its natural rhythm to the period of a small external forcing signal, is a phenomenon that occurs in many real-world systems (e.g. in biological clocks such as circadian cells and cardiac pacemakers [1]). Optimal conditions for entraining an oscillator have been studied, and methods for achieving entrainment

Optics EXPRESS

with minimum forcing power [2], minimum transient time [3,4], maximum coherence [5], and widest locking range [6] have been demonstrated.

Here we use a well-known laser system that displays a rich variety of dynamical behaviors (a semiconductor laser with optical feedback [7–11]) as a testbed to study entrainment experimentally. The laser operates in the so-called *low frequency fluctuations* (LFFs) regime, in which the output intensity displays abrupt dropouts. A typical time trace of the laser intensity in the LFF regime is shown in Fig. 1. The intensity dropouts, which have a spike-like shape, will be referred to as optical spikes. The statistical properties of the spikes and the underlying physical mechanisms have been extensively investigated [12–25], and simulations of the Lang and Kobayashi model [26] have shown that the origin of the optical spikes can be deterministic or stochastic [27–30].

By periodically modulating the laser current it is possible to entrain the spikes to the current modulation [31–33]. Depending on the modulation amplitude and the relation between the modulation frequency, f_{mod}, and the external-cavity frequency, $f_{ext} = c/2L$ (with L being the length of the external cavity), different dynamical regimes have been observed, including quasi-periodicity and frequency locking in Arnold tongues with ratios $f_{mod}/f_{ext} = p/q$ ordered accordingly to the Farey tree hierarchy [34,35]. On the other hand, when the modulation frequency matches the natural frequency of the spikes (without modulation), regular spiking at the frequency of the sinusoidal modulation was reported [36], a phenomenon that was interpreted as due to stochastic resonance [37]. More recently, several of us studied experimentally the entrainment produced by *small-amplitude* sinusoidal current modulation (the peak-to-peak amplitude was less than 2% of the dc value) [38,39]. We characterized the statistics of the time intervals between consecutive spikes (the inter-spike-intervals, ISIs) and used a symbolic method of time series analysis to detect temporal correlations in the ISI sequence. Locking regimes were identified when the ISI probability distribution function (pdf) had a main peak at an integer multiple of the modulation period, T_{mod}. For example, when one spike was emitted in each modulation cycle (1:1 locking), the ISI pdf had a main peak at T_{mod}; however, the large width of the peak, as well as the presence of side peaks, revealed that the timing of the spikes was actually very irregular, i.e., small-amplitude sinusoidal current modulation produced very "noisy" locking.

Here we address the following question: is it possible to obtain, with small-amplitude current modulation, a regular sequence of spikes? To address this issue, we first propose three measures to quantify the quality of the entrainment, and then use them to compare the entrainment produced by three modulation waveforms (pulsed-up, pulsed-down, and sinusoidal). We also characterize the impact of several experimental control parameters: the dc value of the laser current, which controls the natural (un-modulated) spike frequency, the modulation frequency, and the modulation amplitude.

2. Experimental setup

The experimental setup is as in [38,39]. A 685 nm semiconductor laser (AlGaInP multi-quantum well Thorlabs HL6750MG), with solitary threshold current $I_{th,sol}$ = 26.62 mA has part of its output intensity fed back to the laser cavity by a mirror. The length of the external cavity is L = 70 cm which gives a feedback delay time of about 5 ns. The temperature and current were stabilized with an accuracy of 0.01 C and 0.01 mA, respectively. During the experiments the temperature was set to T = 18 C. The optical feedback strength was also kept constant and produced a 7.2% threshold reduction (I_{th} = 24.70 mA). A 90/10 beam-splitter in the external cavity sends light to a photo-detector (Det10A/M Silica based photodetector) that is connected to an amplifier (Femto HSA-Y-2-40) and a 1 GHz digital storage oscilloscope (Agilent Technologies Infiniium DSO9104A).

To modulate the laser current we used a 500 MHz Bias-T in the laser mount. Three different waveforms, generated by a function generator (Agilent 81150A Pulse Function Arbitrary Noise Generator), were investigated: pulse-up, pulse-down and sinusoidal. The duration of the pulse

Optics EXPRESS

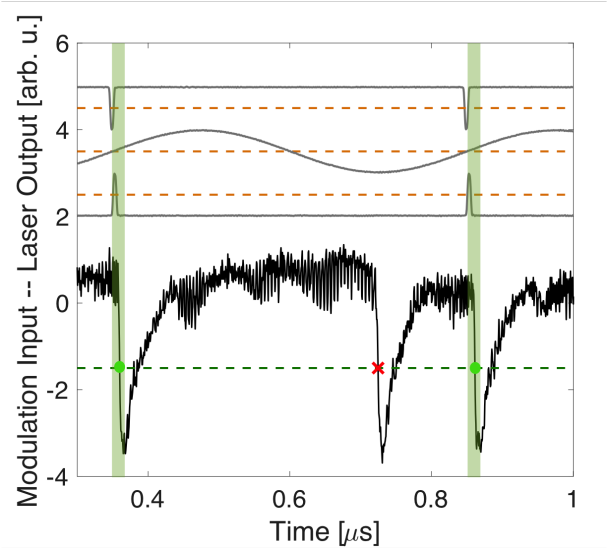

Fig. 1. Time series of the laser intensity (black line, normalized to zero mean and unit variance) and time series of the pump current (gray lines, different waveforms are shifted vertically for clarity). The dashed green line indicates the threshold used, -1.5, for detecting the spikes in the intensity signal. The dashed orange lines indicate the threshold used, in the pump current signal, to define the start of the detection window of τ = 15 ns, indicated as vertical green shaded areas (see text for details). The spikes occurring within the detection window (green dots) are counted in the success rate, Eq. (1); the spike that occurs outside (red cross) is counted in the false positive rate, Eq. (2).

was the shortest available from the function generator: 5 ns with raising and falling times of 2.5 ns each.

A LabVIEW program was used to control the experiment. The dc value of the pump current was varied from 25 mA to 29 mA in steps of 0.5 mA. As discussed in [40, 41], for the lowest and for the highest pump current values the spikes are not well defined as the intensity dynamics is noisy and irregular. In contrast, well-defined spikes occur for pump currents in the range 25.5–27.5 mA, where the natural spike frequency (without modulation) varies in the range 3–30 MHz (see in [42] a video showing how the intensity dynamics gradually changes as the pump current increases). The modulation frequency, f_{mod}, was varied from 1 MHz to 80 MHz in 79 steps of 1 MHz each. The peak to peak modulation amplitude was varied from 0.19 to 0.631 mA in 7 steps of 0.063 mA . Therefore, the modulation amplitude, for the lowest dc value of the pump current, 25.5 mA, represents a variation between 0.75% and 2.53% of the dc level, while for the highest dc value, 27.5 mA, it represents a variation between 0.65% and 2.53%. We remark that the current is not modulated near threshold, but at a current level relative to the threshold equal to I/I_{th}=1.01 for the lowest dc value, and I/I_{th}=1.17 for the highest dc value.

For each set of parameters (dc pump current, modulation frequency and modulation amplitude), $N = 10^7$ data points were recorded with a sampling rate of 2 GS/s (temporal resolution of 0.5 ns), allowing an observation time of 5 ms. It is important to note that the intensity dropouts are the envelope of fast, pico-second pulses, which can be detected by using a much faster detection system [14]. Since we are interested in the entrainment of the slower spiking dynamics, the detection bandwidth experimentally available is enough for our purposes.

We analyze the time series of the laser intensity (see Fig. 1) and detect the spike times with

Optics EXPRESS

the same method as in [40,41]. First, the intensity time series, which has mean value equal to zero due to the amplifier, is normalized to unit variance. Then, a spike is detected whenever the intensity drops below a given value. As in [40,41] we use a threshold of −1.5 in units of the standard deviation, indicated with a green dashed line in Fig. 1). To avoid detecting as spikes the fluctuations that occur during the recovery process, the intensity has to grow above the zero mean value, before another spike can be detected.

The start of the time window to detect and quantify the laser response to the current perturbation (as described in Sec. 3) is defined by using a threshold in the pump current signal: for the pulsed (up and down) waveforms, the window starts when the current signal grows above half the perturbation amplitude; for the sinusoidal signal, the window starts when the current signal grows above the mean value. These thresholds are indicated with orange dashed lines in Fig. 1, where we also show two spikes that occur within the time interval τ (indicated with green dots), and one spike that occurs outside (red cross). Regarding the window length, τ, it should not be too long or too short: if it is too short, the laser does not have enough time to emit a spike while on the other hand, if τ is too long, the laser can emit more than one spike in the interval τ. As the smallest duration of a spike is about 10 ns, the duration of the window τ was chosen equal to 15 ns (so two spikes can not occur in the same window), except when the modulation period is shorter than 15 ns (i.e., when $f_{mod} > 67$ MHz). In this case no window is used. A sensitivity analysis was performed to analyze the influence of τ (see Fig. 6).

3. Quantification of the entrainment quality

In this section we propose three measures to capture complementary aspects of the quality of the entrainment of the optical spikes to the external periodic signal applied to the laser current: the "success rate" (SR, which can also be referred to as true positive rate), the "false positive rate" (FPR), and the "coefficient of variation" (C_V).

The success rate measures the response of the laser per modulation cycle: if the laser emits one spike each cycle, SR=1, if it emits one spike every two cycles, SR=0.5, etc. A drawback of this simple definition is that it does not take into account the regularity of the timing of the spikes: the spikes could be emitted at any phase of the modulation cycle, or at a well-defined phase. Therefore, we use a detection window, τ, and count the spikes emitted within this interval of time (see Fig. 1). As it will be discussed below, for capturing the regularity of the generated spikes, the start and the duration of the detection window need to be chosen appropriately. Taking into account the time window, τ, during which the laser is expected to respond to the current modulation by emitting a spike, the "success rate" is defined as

$$\mathrm{SR}(\tau) = \frac{\#\text{ of spikes emitted in the interval } \tau}{\#\text{ of modulation cycles}}. \tag{1}$$

Complementing this measure, the "false positive rate" measures the spikes which are emitted outside this window,

$$\mathrm{FPR}(\tau) = \frac{\#\text{ spikes that are not emitted in the time interval } \tau}{\text{Total }\#\text{ of spikes}}. \tag{2}$$

FPR=0 indicates that the spikes are always emitted within the time interval τ, while FPR=1 indicates that the laser does not emit any spike within the time interval τ. We note that the number of modulation cycles and the number of spikes in the intensity time series (either "natural" or induced by the current modulation) can not be equal to zero. As we capture the intensity dynamics during 5000 μs ($N = 10^7$ data points with 0.5 ns temporal resolution) and for our experimental conditions the inter-spike-interval is typically < 1 μs, the intensity time series always contains a large number of spikes. The smallest modulation frequency is 1 MHz, and therefore, the number of modulation cycles is ≥5000.

Optics EXPRESS

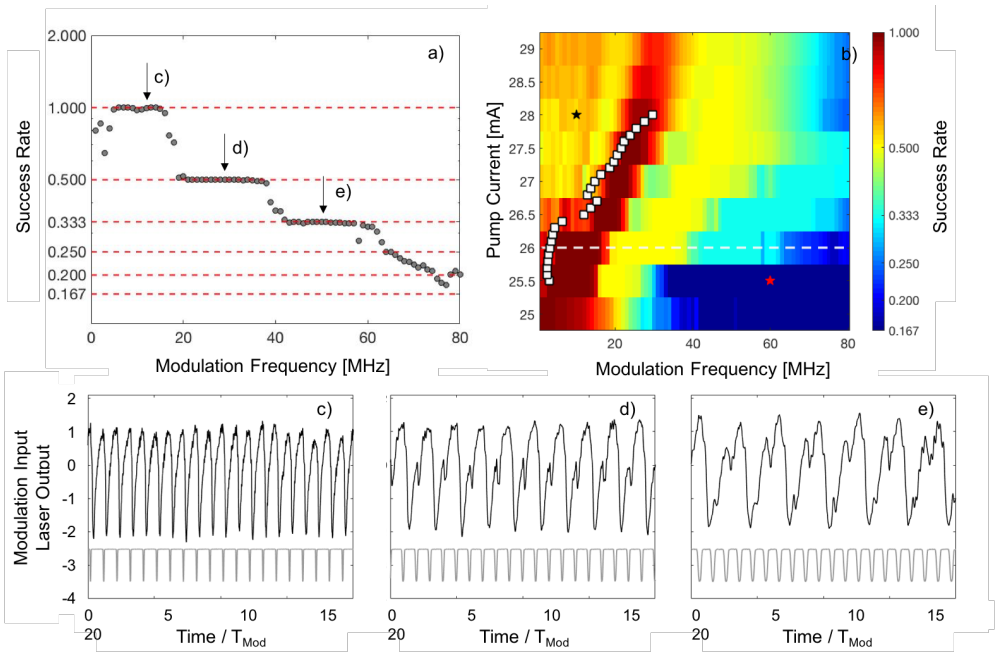

Fig. 2. Entrainment of the spikes in the laser intensity, when a periodic signal with pulse-down waveform is used to modulate the laser current. The modulation amplitude is 2.4% of the dc value of the pump current, I_{dc}. (a) Success rate, Eq. (1), in log scale, as a function of the modulation frequency, f_{mod}, when I_{dc} = 26.0 mA. The horizontal dashed lines indicate the value expected, SR = $1/n$, for locking n : 1, with $n = 1, 2 \ldots$. The arrows indicate the value of f_{mod} corresponding to the time series shown in panels (c), (d) and (e). (b) Success rate (in color code) as a function of f_{mod} and I_{dc}. The white squares indicate the natural (un-modulated) spike frequency, for the range of values of I_{dc} where the spikes, without modulation, have a well-defined frequency [40, 41]. The white dashed line indicates the SR horizontal cut shown in panel (a). The symbols indicate the different regions discussed in the text, and the corresponding time series are displayed in Fig 3. Panels (c), (d) and (e) display locking 1:1, 2:1 and 3:1 for f_{mod} = 14 MHz, 30 MHz, and 50 MHz respectively.

Perfect 1:1 locking occurs when the laser emits, for each modulation cycle, only one spike, and it is emitted within the time interval τ. In this case, SR=1 and FPR=0. For 2:1 locking, if all the spikes are emitted within the time window τ, SR=0.5 and FPR=0.

The third measure used, the "coefficient of variation", quantifies the overall regularity of the timing of the spikes. It is defined as the ratio between the standard deviation, σ_{ISI}, and the mean value, $\langle I \rangle$, of the sequence of inter-spike-intervals, $\{\ldots I_i = t_{i+1} - t_i \ldots\}$, where t_i are the spike times:

$$C_V = \frac{\sigma_{ISI}}{\langle I \rangle}. \tag{3}$$

Note that $C_V = 0$ indicates perfectly regular spike timing: $\sigma_{ISI} = 0$ means that the time intervals between consecutive spikes, $\{\ldots I_i \ldots\}$, are all equal.

4. Results

We first fix the dc value of the pump current (I_{dc} = 26.0 mA), the modulation amplitude (2.4% of I_{dc}), and the modulation waveform (pulse-down) and vary the modulation frequency, f_{mod}. Figure 2(a) displays the SR (in log scale) where we observe, as f_{mod} increases, three well-defined

Optics EXPRESS

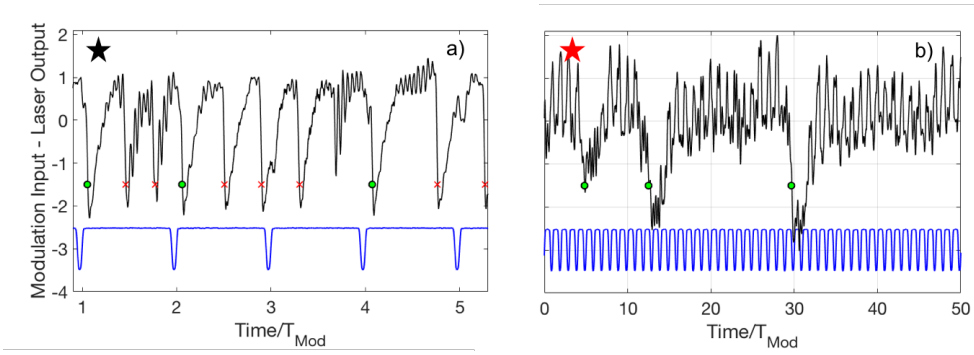

Fig. 3. Modulation input and laser output time series to illustrate dark yellow and dark blue areas detailed in Fig. 2(b). (a) Case example for the dark yellow area I_{dc} = 28.00 mA and f_{mod} = 10 MHz (black star in Fig. 2b). (b) Case example for the dark blue area, I_{dc} = 25.50 mA and f_{mod} = 60 MHz (red star in Fig. 2b).

plateaus where SR is equal to 1, 1/2 and 1/3 (i.e. lockings 1:1, 2:1 and 3:1 respectively). The corresponding time series, depicted in Figs. 2(c-e), show that the spiking is quite regular.

Figure 2(b) displays in color code the SR as a function of I_{dc} and f_{mod}. As we move along the horizontal dashed line [which corresponds to the parameters in Fig. 2(a)] the region with SR = 1 (red) is followed, as f_{mod} increases, by a region where the SR = 1/2 (yellow), which is followed by a region where SR = 1/3 (light blue). If f_{mod} is increased further, SR continues to decrease (darker blue). The red and yellow regions cover a wide parameter region; however, if I_{dc} is too high, in the red region SR is less than 1, indicating that the quality of the locking decreases. We interpret this as due to the fact that, for high pump currents the internal dynamics tends to dominate over the weak external modulation.

In Fig. 2(b) we also show the natural spike frequency (when the laser is not modulated, marked by white squares) for the range of values of I_{dc} where the spikes, without modulation, have a well-defined frequency [40, 41], and one can see that the natural spike frequency is clearly correlated to the onset of locking 1:1.

For high enough I_{dc} and slow enough modulation [dark yellow area in the top left corner of Fig. 2(b)] the frequency of the spikes is faster than the modulation frequency (a typical time series is shown in Fig. 3(a). In this case many spikes are not induced by the current pulse-down perturbations. On some occasions a perturbation occurs just after the spike is emitted and thus within the recovery refractory time interval during which another spike can not be triggered. Therefore, in this region, SR is low while the FPR is high (it grows up to almost one as I_{dc} increases, because the spiking dynamics becomes faster). In the opposite corner (for high modulation frequencies and low pump currents) the success rate is very low (dark blue), and this can be understood by an inspection of a typical intensity time series, shown in Fig. 3(b). We see that the current perturbations are too fast, and fail to produce spikes.

4.1. Comparison of modulation waveforms

Next, we analyze the impact of the waveform used to entrain the laser spikes. In Fig. 4 we compare the three measures proposed in Sec. 3 (SR, FPR and C_V), as a function of I_{dc} and f_{mod}. In the case of pulsed modulation (either up or down), locking regions 1:1, 2:1, and 3:1 are revealed by red, yellow and light blue areas in the SR plots, Figs. 4(a) and (c). Even though no qualitative differences are observed between both pulsed waveforms, the regions where locking is achieved are broader when the pulse-down waveform is applied. This could be due to the fact that the shape

Optics EXPRESS

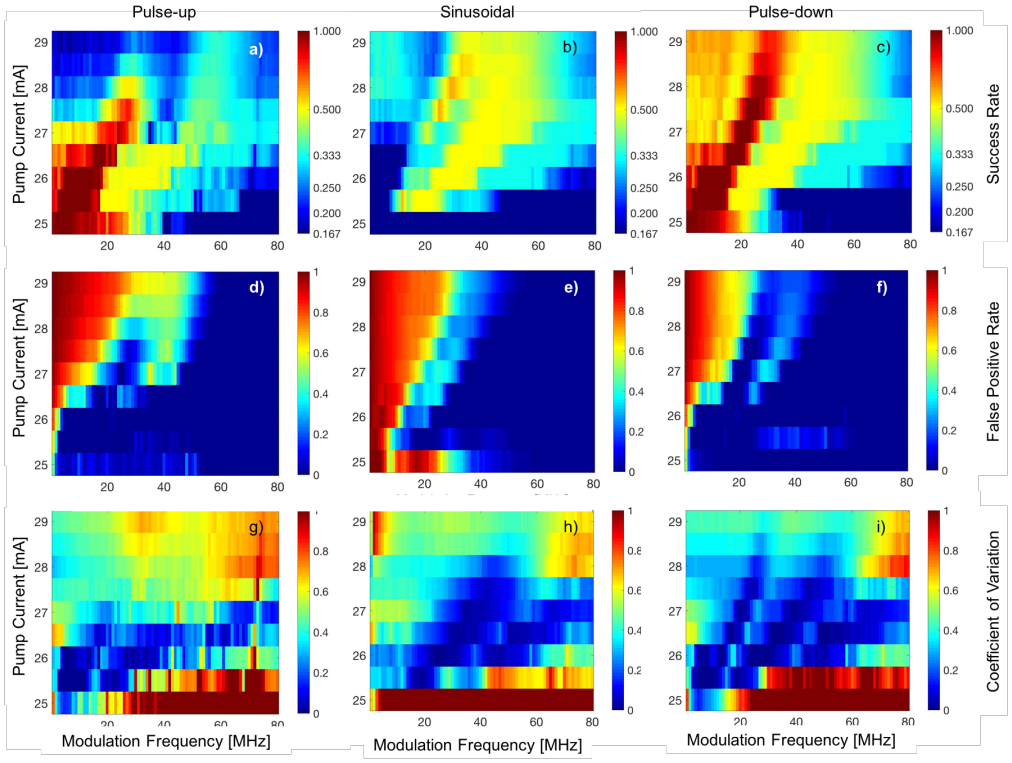

Fig. 4. Success rate (a,b,c), false positive rate (d,e,f) and coefficient of variation (g,h,i) in color code for the three waveforms studied, vs. the modulation frequency (in the range 1 – 80 MHz) and the dc value of the laser current. The modulation amplitude is 0.65 mA, which corresponds to 2.5% (2.2%) for I_{dc} = 25 mA (29 mA).

of the response (a dropout) is similar to the shape of the perturbation (pulse-down waveform).

In contrast, a remarkable difference is seen in Fig. 4(b) with the sinusoidal waveform: locking 1:1 is not detected. For higher frequencies, the locking regions 2:1, and 3:1 (yellow and light blue areas) are similar to the ones seen with the two pulsed waveforms.

In the FPR plots, Figs. 4(d-f) we note that for low modulation frequencies and high pump currents (left upper corner of the plots) a large number of spikes are counted as false positives. This is due to the fact that the modulation period is long and many spikes can occur outside the detection window (an example is shown in Fig 3(a)). When increasing f_{mod} while keeping constant I_{dc}, the FPR decreases gradually as the first locking region, 1:1 or 2:1 depending on the modulation waveform, is reached.

In Figs. 4(d) and (f) an interesting feature is uncovered during the transition from locking 1:1 to 2:1, which occurs when f_{mod} increases while I_{dc} is kept constant: in between the locking regions, the FPR increases (note the light blue region in between the dark blue regions). This effect is due to the reorganization of the spikes, which no longer fit in one period (as in the 1:1 region) but two periods is too long for a single spike (as in the 2:1 region). Therefore, in the transition from 1:1 to 2:1 locking, many spikes do not occur within the detection window, and thus, are counted as false positives. In contrast, for the sinusoidal waveform, Fig.4(e), locking 1:1 is not achieved and thus, the FPR decreases gradually until 2:1 locking is reached. As discussed in Sec. 3, with further increase of f_{mod} above 67 MHz (i.e. when the modulation period is shorter

Optics EXPRESS

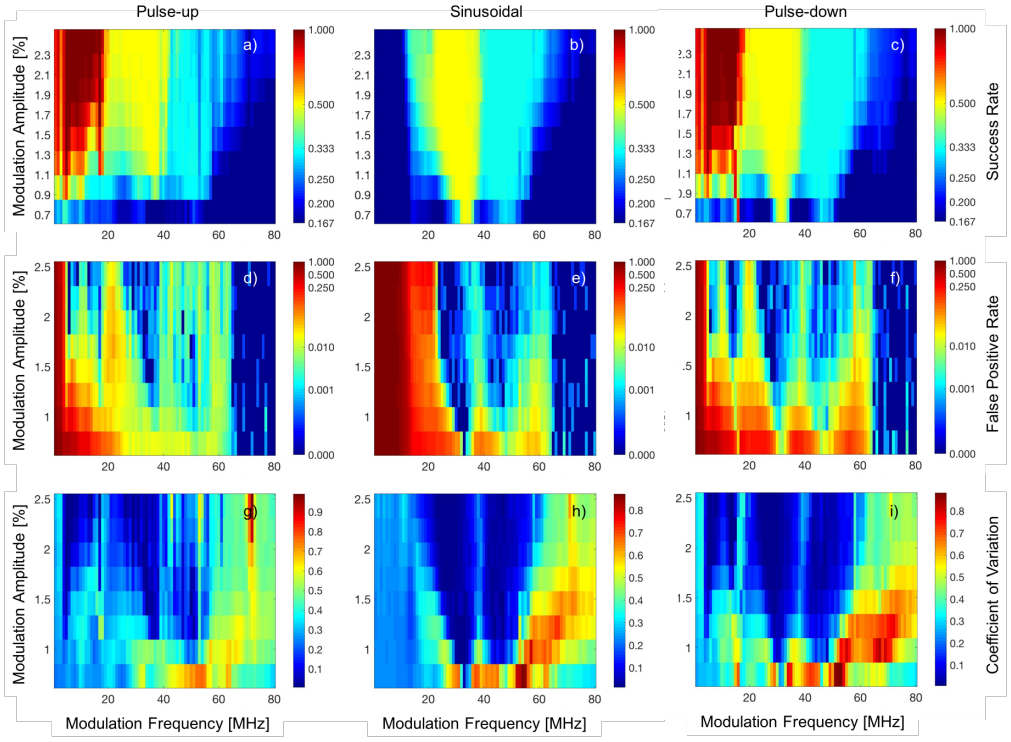

Fig. 5. Success rate (a,b,c), false positive (d,e,f) and coefficient of variation (g,h,i) for different modulation amplitudes for the three input modulation studied. (a, d, g) pulse-up, (b, e, h) sinusoidal and (c, f, i) pulse-down waveforms. The dc value of the pump current is I_{dc} = 26.0 mA. For this dc current value and a modulation amplitude of 0.65 mA (which represents 2.5% of I_{dc}), locking regions 1:1, 2:1 and 3:1 are observed in Fig. 4.

than the detection window), FPR= 0.

Figures 4(g)-(i) display the coefficient of variation, in color plot. C_V captures the regularity of the timing of the spikes and is close to zero in the locking regions (dark blue areas) where the spikes are entrained to the periodic current modulation. When comparing the three panels we observe that the pulse-down waveform is more efficient to entrain the spikes since the dark blue areas are larger. When a pulse-up waveform is applied we observe entrainment in most of the modulation frequencies studied, but within a narrower region of pump currents, in comparison with the pulse-down waveform. When a sinusoidal waveform is applied, entrainment is not observed for frequencies below ~10 MHz: the light blue color in Fig. 4(f) for 25.5-26 mA corresponds to $C_V \sim 0.2 - 0.3$, which indicates heterogeneous distribution of the timing of the spikes (i.e., noisy entrainment, as reported in [38]); in contrast, in Figs. 4(g) and 4(i) the dark blue corresponds to $C_V \sim 0$. At higher frequencies the laser response is similar to the one observed with the pulsed modulation (up or down) showing locking regions 2:1 and 3:1.

4.2. *Influence of the modulation amplitude*

Next, we analyze the role of the modulation amplitude in the entrainment quality. As seen in Figs. 5(a)-(c), when the modulation amplitude is larger than ~ 1% and the modulation frequency is not too fast (less than 60 MHz), the laser responds to the input signal with SR close to 1, 1/2 or 1/3, depending on f_{mod}. The FPR plots, displayed in Figs. 5(d)-(e), reveal that if the modulation

Optics EXPRESS

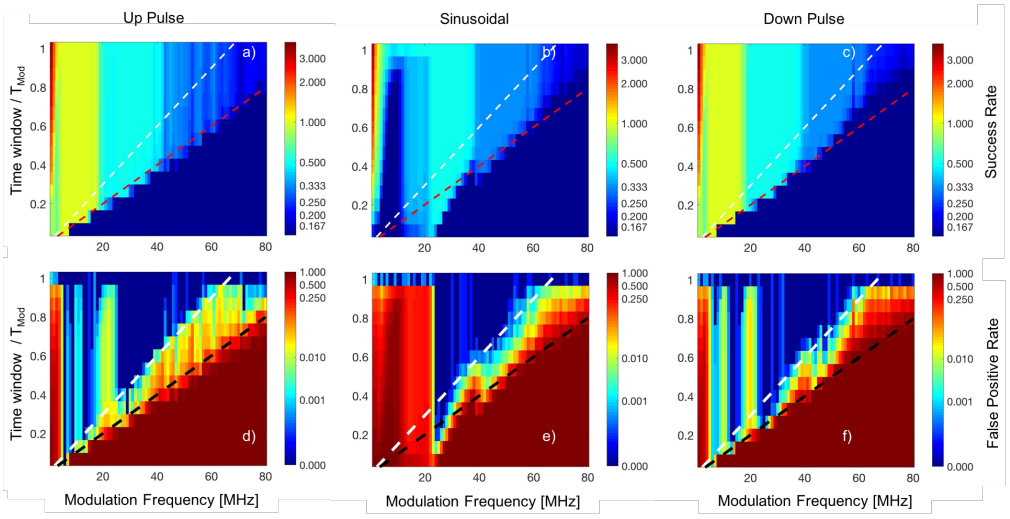

Fig. 6. Success rate and false positives rate as a function of the modulation frequency and of the detection time window, normalized to the modulation period. The modulation waveform is (a,d) pulse-up, (b,e) sinusoidal and (c,f) pulse-down. Black and white dashed lines represent τ = 10 ns and τ = 15 ns respectively. The dc value of the pump current is I_{dc} =26.0 mA and the modulation amplitude is 2.43% of I_{dc} (0.65 mA) because for these values, locking regions 1:1, 2:1 and 3:1 are observed in Fig. 4.

amplitude is large enough (larger than 1%-1.5% depending on the modulation frequency and waveform), there are no spikes outside the detection window. As in Figs. 4(d) and (f), here we also note that in between two locking regions, the FPR is not zero.

To observe locking 1:1 with pulse-up or pulse-down waveforms, a minimum 2% amplitude has to be applied, while for the sinusoidal modulation, 1:1 is not produced, at least for the range of small amplitudes used in this work. On the other hand, locking 2:1 and 3:1 require smaller amplitudes, with any of the three waveforms studied.

4.3. *Influence of the window length*

So far we have calculated the SR and the FPR using a detection window of τ = 15 ns, except when the period of the modulation is shorter than 15 ns, in which case, no detection window is used. Here we perform a sensitivity analysis to evaluate the role of the detection window. For each modulation frequency, we vary τ/T_{mod} between 0.1 and 1. Figure 6 displays the SR and the FPR as a function of f_{mod} and τ/T_{mod}, for the three waveforms studied. The black and white dashed lines indicate τ = 10 ns and 15 ns respectively. We note that when τ < 10 ns (i.e., below the black dashed line) SR~ 0 and FPR~ 1, for all frequencies and waveforms. This is due to the fact that the detection window is too short, and most of the spikes occur outside the window. As expected, the pulse-up and pulse-down plots are similar, while the sinusoidal plots show significant differences.

We first consider the pulsed waveforms. In the SR plots (top row), for fixed modulation frequency, when τ/T_{mod} increases above the dashed line, the SR becomes independent of the window length, and we note well-defined regions: for low f_{mod}, (<3 MHz) SR>1 (red), which is due to the fact that the detection window is long and more than one spike can occur in the window; for higher f_{mod} (>5 MHz), SR~1 suggests 1:1 locking, followed by SR~ 1/2 (2:1) and SR~ 1/3 (3:1).

Optics EXPRESS

In the FPR plots (bottom row) we note that when τ/T_{mod} increases above the white dashed line that represents τ = 15 ns, the FPR becomes nearly independent of the window length; in the locking regions FPR$\sim$ 0 while FPR is not zero in between the locking regions. FPR$\sim$ 1 if τ/T_{mod} is small because most of the spikes occur outside the detection window, and gradually decreases to 0 as $\tau/T_{mod} \rightarrow 1$, because in this limit the detection window covers the whole modulation cycle.

We note that, if $\tau > 15$ ns (above the white dashed line) in the locking regions FPR$\sim$ 0, and therefore, we have used this value for the analysis. We note however that, in the plots obtained for the sinusoidal waveforms, the lines τ = 10 ns and τ = 15 ns do not correspond to any sharp change in the SR or FPR values, and we also note that the 1:1 locking is not detected, for any value of τ/T_{mod}; however, for the sinusoidal waveform the transition to 2:1 locking is very well defined (occurs at a frequency slightly above 20 MHz) and the locking is very robust as SR = 1/2 and FPR = 0 even when the detection window is very short ($\tau/T_{mod} \sim 0.1$). The transition to 3:1 locking occurs at a frequency close to 40 MHz, consistent with the two pulsed waveforms. Summarizing, main differences between the three waveforms are seen at low frequencies, while if the modulation is fast enough, the waveform used has less impact on the SR and FPR values.

5. Conclusions and discussion

We have studied experimentally entrainment phenomena in a semiconductor laser with optical feedback with small-amplitude pump current modulation. The feedback conditions are such that the laser operates in the low-frequency fluctuations regime, where the intensity displays abrupt dropouts, which are referred to as optical spikes, and can be entrained to the current modulation. We have compared three modulation waveforms (pulse-up, pulse-down and sinusoidal), and analyzed the effects of varying the modulation frequency and amplitude, and the dc value of the pump current. The entrainment quality was quantified by using three measures which provide complementary information: the success rate (SR) measures the spikes that occur within a detection window τ, the false positive rate (FPR) measures the additional spikes that occur outside the detection window, and the "coefficient of variation" measures the overall regularity of the timing of the spikes.

Locking regions 1:1, 2:1 and 3:1 were identified; in these regions SR = 1, 1/2 and 1/3 respectively, while the FPR and the C_V were close to zero. Regarding the role of the laser current, we found that the spikes are easier to entrain when the laser is operated at intermediate pump currents, i.e., not too close to the threshold, and not too close to the coherence collapse. We interpret this observation as due to the fact that, if the pump current is too close to the threshold, the laser dynamics is dominated by noise, and no well-defined spikes can be entrained to the modulation; on the other hand, if the pump current is too high, the internal dynamics of the laser tends to dominate over the weak current modulation.

With the sinusoidal waveform and the small modulation amplitudes considered here (up to 2.5%) we found that the laser does not show 1:1 entrainment. We have also found that, with the pulse-up waveform, the locking regions are smaller than with the pulse-down waveform. Regarding the response time, we have found that is about the same for the three waveforms: if $\tau < 10$ ns the success rate decreases drastically as no modulation waveform or modulation parameters are capable of producing a fast response. This "delay" is due to the finite response time of the laser, and seems to be independent of the modulation waveform and of the operation conditions.

Summarizing, for our experimental conditions the pulse-down and sinusoidal waveforms have similar performance for producing 2:1 locking: the laser responds to the periodic modulation by emitting a regular sequence of spikes, characterized by SR = 1/2 and very small values of FPR and C_V. On the other hand, if we are interested in maximizing the success rate (i.e., in obtaining one spike per modulation cycle, SR = 1) then the pulse-down waveform is the most convenient,

Optics EXPRESS

as SR= 1 accompanied by small FPR and C_V values, is achieved in a wider parameter region. As future work, it will be interesting to extend this study to aperiodic, information-carrying signals. Even through it is an open question how the results obtained here can be translated to other systems, we speculate that, regarding laser diodes, the best current perturbation waveform has a similar shape as the intensity pulse to be generated (here, optimal 1:1 locking is observed when each pulse-down current perturbation is shortly followed by an abrupt intensity dropout). This observation is consistent with recent theoretical work that has shown that, in an optical injection configuration, a pulse-up current perturbation can generate a high intensity pulse, while a pulse-down perturbation is unlikely to generate a pulse [43]. These findings could be relevant for diode lasers used for sensing applications: if the laser operating conditions can be tuned to the parameter region where "natural" dropouts are rare, then the laser can respond to a small decrease of the pump current with an abrupt intensity dropout (i.e., the operating parameters –pump current, feedback strength, delay time– are tuned such that the success rate is maximized while the false positive rate is minimized).

Funding

Spanish MINECO FIS2015-66503-C3-2-P; ICREA ACADEMIA, Generalitat de Catalunya.